

## PLANT SCIENCES

# Phosphorylation at serine-260 of Toc33 is essential for chloroplast biogenesis

Yuan-Chi Chien<sup>1,2</sup> and Gyeong Mee Yoon<sup>1,2\*</sup>

**Chloroplast biogenesis, essential for photosynthesis, depends on the import of nuclear-encoded proteins through the translocon at the outer envelope of chloroplasts (TOC) complexes. Despite its importance, the mechanisms regulating this process remain largely elusive. We identify serine-260 (S260) as a critical phosphorylation site in Toc33, a core TOC component. This phosphorylation stabilizes Toc33 by preventing its ubiquitination and degradation. Constitutive triple response 1 (CTR1), a negative regulator of ethylene signaling, and its paralog RAF-like kinase are involved in phosphorylating Toc33. Disruption of Toc33 phosphorylation impairs its stability and photosynthetic protein import, consequently affecting chloroplast structural integrity and biogenesis. Our findings underscore the essential role of TOC phosphorylation in chloroplast biogenesis and reveal an unexpected regulatory network involving RAF-like kinases in organelle development.**

## INTRODUCTION

Photosynthesis in plants traces its origin to an endosymbiotic event with cyanobacteria. Over evolutionary time, most ancestral chloroplast genes were transferred to the nuclear genome, necessitating the post-translational import of proteins via the translocon at the outer envelope of chloroplasts (TOC) and translocon of the inner envelope of chloroplasts (TIC) machinery (1, 2). Chloroplast biogenesis and photosynthetic capacity depend on the stability, activity, and assembly of the TOC complex. This complex consists of Toc34 family proteins (Toc33 and Toc34), Toc159 family proteins (Toc159, Toc120, Toc90, and Toc132), and Toc75 protein channel (1). Within this complex, Toc33, a key guanosine triphosphatase (GTPase), plays an indispensable role in the recognition and binding of nuclear-encoded chloroplast preproteins, as evidenced by the distinct pale-green phenotype of the Toc33 mutant *ppi1* (plastid protein import 1) (3). The Toc33 function is modulated by post-translational modifications (PTMs). During chloroplast developmental transition and stress, Toc33 undergoes ubiquitination and degradation by SP1 (suppressor of *ppi1*), a RING-type E3 ligase, its close homolog SPL1-like 1 (SPL1), and SPL2 (4–6). These E3 ligases are components of the chloroplast-associated protein degradation (CHLORAD) system, which functions as a ubiquitin-based protein degradation pathway targeting chloroplast outer envelope membrane proteins, including components of the TOC complex. Toc33 function is also modulated by SUMOylation, as mutants deficient in SUMO conjugation pathways suppress *ppi1* phenotypes, leading to increased TOC protein levels and improved chloroplast development (7). Conversely, SUMOylation of Toc159 partially stabilizes it against the ubiquitin-proteasome pathway (8). Phosphorylation is another critical regulation that influences Toc33 GTP binding and dimerization (9–11). Despite these insights, the biological relevance of Toc33 phosphorylation and the identity of its kinases in planta remain enigmatic (12, 13).

Constitutive triple response 1 (CTR1) is a rapidly accelerated fibrosarcoma (RAF)-like Ser/Thr protein kinase that serves as a negative

regulator in the ethylene signaling, a plant hormonal pathway governing plant growth and stress responses (14). In the absence of ethylene, CTR1 phosphorylates the positive regulator ethylene insensitive 2 (EIN2), promoting its degradation and thereby halting ethylene signal transduction (15, 16). When ethylene binds to the ethylene receptors at the endoplasmic reticulum (ER), CTR1 activity is inhibited, allowing EIN2 to be cleaved. The C-terminal fragment of EIN2 then translocates into the nucleus, where it activates the transcription of ethylene-responsive genes (15–17). Historically, CTR1 was thought to be exclusively localized to the ER through its interaction with the ethylene receptor ethylene response 1 (ETR1) (18, 19). However, recent studies have revealed that CTR1 also localizes to and interacts with proteins in the cytoplasm and nucleus (20–23). Despite these advances, the specific roles of CTR1 in the cytoplasm and the potential ethylene-independent functions of CTR1 remain largely unexplored.

## RESULTS

### CTR1's chloroplast association and interaction with the TOC complex

To investigate the role of CTR1 in the cytoplasm, we examined its subcellular localization in light-grown *Arabidopsis* seedlings. Using both stable transgenic lines expressing green fluorescent protein (GFP)-CTR1 from its native promoter and the *Arabidopsis* protoplast transient expression system, we observed that GFP-CTR1 partially associated with the chloroplast outer envelope membrane (Fig. 1A and fig. S1). Unlike free GFP, which dispersed throughout the cytoplasm and absent in chloroplasts, GFP-CTR1 showed distinct localization at the chloroplast outer membrane when the focal plane was focused on the mesophyll, the region with the highest chloroplast density (fig. S2, A and B). This GFP-CTR1 chloroplast outer membrane localization persisted even when ethylene signaling was inhibited by silver thiosulfate (STS) and in the ethylene-insensitive *ein2-5* mutant (Fig. 1A and figs. S1A and S3), indicating that the chloroplast outer membrane localization of CTR1 is independent of ethylene signaling. Colocalization analyses using stable transgenic lines coexpressing GFP-CTR1 and mCherry-Toc33 (Fig. 1B and fig. S4A), along with a protoplast transient system (fig. S4, B and C) revealed the dual localization of CTR1. When focused on the epidermal

Copyright © 2025 The Authors, some rights reserved; exclusive licensee American Association for the Advancement of Science. No claim to original U.S. Government Works. Distributed under a Creative Commons Attribution NonCommercial License 4.0 (CC BY-NC).

<sup>1</sup>Department of Botany and Plant Pathology, Purdue University, West Lafayette, IN 47907, USA. <sup>2</sup>The Center for Plant Biology, Purdue University, West Lafayette, IN 47907, USA.

\*Corresponding author. Email: yoong@purdue.edu

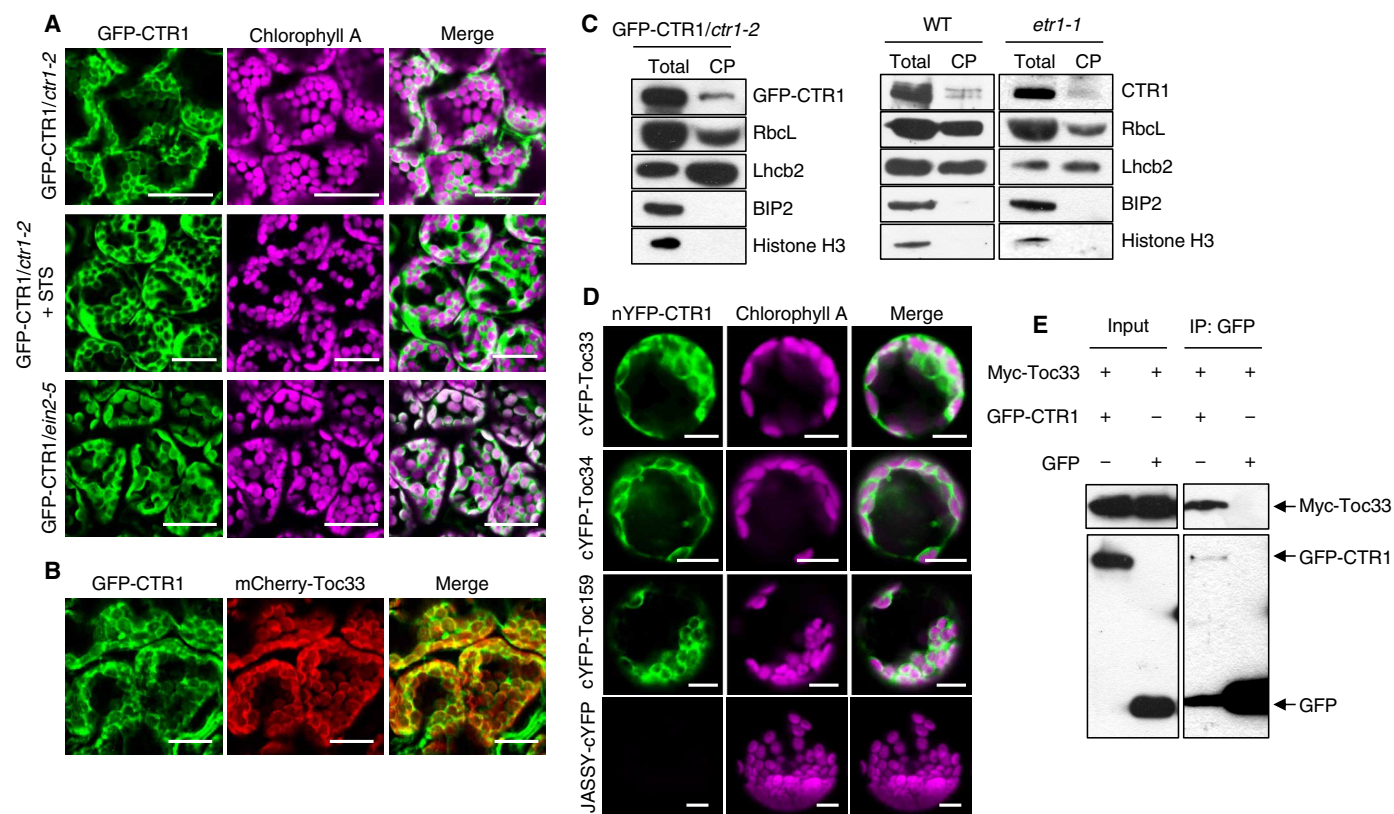


**Fig. 1. CTR1 associates with the chloroplast and interacts with TOC complex proteins at the chloroplast outer envelope.** (A) Localization of GFP-CTR1 at the chloroplast outer membrane in *ctr1-2* *Arabidopsis* seedlings, either untreated or treated with the ethylene inhibitor silver thiosulfate (STS), and in the ethylene-insensitive mutant *ein2-5*. Scale bars, 50  $\mu$ m. (B) Colocalization of GFP-CTR1 and mCherry-Toc33 at the chloroplast outer membrane in a stable *Arabidopsis* transgenic line. Scale bar, 50  $\mu$ m. (C) GFP-CTR1 or endogenous CTR1 are localized in isolated chloroplasts (CP) from *GFP-CTR1/ctr1-2* transgenic lines, WT, or *etr1-1* plants. Immunoblot was done using an anti-GFP antibody for the transgenic line and an anti-CTR1 antibody for either WT or *etr1-1*. (D) CTR1 showed proximity to the TOC complex proteins (Toc33, Toc34, and Toc159) in BiFC assays using *Arabidopsis* protoplasts. JASSY, a chloroplast outer membrane protein, was used as a negative control. Scale bars, 10  $\mu$ m. (E) In vivo interaction between GFP-CTR1 and Myc-Toc33 was assessed through coimmunoprecipitation using *Arabidopsis* protoplasts, with GFP serving as a negative control.

layer, GFP-CTR1 was observed in the cytoplasm, consistent with the prior studies (14, 18, 20). At the mesophyll focal plane, GFP-CTR1 colocalized with mCherry-Toc33, a known chloroplast outer membrane protein (fig. S4, A and B), and its fluorescent signal was detected at the outer membrane of chloroplasts expressing stroma-targeting Rubisco small subunit (RbcS) transit peptide-fused mCherry (RbcS-TP-mCherry) (fig. S4C). Supporting these cell biological observations, both GFP-CTR1 and endogenous CTR1 were detected in isolated chloroplasts from transgenic plants, wild-type (WT), and ethylene-insensitive *etr1-1* mutant (Fig. 1C), while free GFP was absent in isolated chloroplasts (fig. S2C). Moreover, treating isolated chloroplasts with thermolysin, a protease that digests proteins exposed on the organelle surface, removed the majority of chloroplast-associated GFP-CTR1 (fig. S2D), demonstrating its association with the chloroplast outer membrane. Notably, the observed GFP-CTR1 signals at the plasma membrane in protoplasts (fig. S4, B and C) align with proximal labeling studies identifying nonphotosynthetic hypocotyl 3, a plasma membrane-localized phototropism regulator, as a CTR1-interacting protein (21). Together, these results demonstrate that CTR1 localizes to the chloroplast outer membrane in addition to its previous known localizations in the cytoplasm and nucleus (14, 18, 20, 22).

Given the structural similarity between CTR1 and the mammalian RAF kinases, which interact with Ras GTPase (24), we investigated whether CTR1 interacts with the TOC complex proteins, specifically those with a GTPase domain such as Toc33, Toc34, and Toc159, key preprotein-binding GTPases located at the chloroplast outer membrane. Bimolecular fluorescence complementation (BiFC) assays revealed that CTR1 is in proximity with Toc33, Toc34, and Toc159 at the chloroplast outer envelope membrane (Fig. 1D and fig. S5). In contrast, JASSY (25), another chloroplast outer membrane protein, showed no reconstituted yellow fluorescent protein (YFP) signal in the BiFC assay with CTR1, suggesting that CTR1 is specifically in proximity to the TOC proteins (Fig. 1D and fig. S5). In addition, coimmunoprecipitation assays demonstrated that Myc-Toc33 is pulled down together with GFP-CTR1, but not free GFP, further supporting that CTR1 forms a structural complex with Toc33 in vivo (Fig. 1E).

#### Analysis of CTR1's effect on TOC proteins

To elucidate the role of CTR1 in regulating TOC proteins, we first assessed its impact on Toc33 protein localization. GFP-Toc33, stably expressed in both WT and *ctr1-2* null mutant, displayed similar localization at the chloroplast outer membrane (fig. S6A). We then

compared endogenous Toc33 protein levels across WT, *ctr1-2*, and a CTR1 overexpression line (CTR1-ox). Despite similar *Toc33* mRNA levels in these lines (fig. S6B), Toc33 protein levels were reduced in *ctr1-2* and elevated in CTR1-ox seedlings (Fig. 2A and fig. S7). Consistent with previous reports, Toc33 levels increased in the *sp1-1* mutant, but remained unchanged in ethylene-insensitive mutants, such as *etr1-1*, *ein2-5*, and *ein3/eil1* (Fig. 2B). These data collectively suggest that Toc33 abundance is regulated through a mechanism independent of the ethylene signaling, but dependent on CTR1 (Fig. 2, A and B). Treatment of *Arabidopsis* protoplasts with cycloheximide, a protein synthesis inhibitor, revealed that GFP-Toc33 degrades with a half-life of approximately 2 hours (Fig. 2C). However, GFP-Toc33 remained stable for up to 3 hours in the presence of co-expressed Myc-CTR1, indicating that CTR1 stabilizes Toc33 (Fig. 2C). The stabilizing effect was observed for both Toc33 and its close paralog Toc34, even in the absence of ETR1 (Fig. 2, D and E), supporting that CTR1 regulates Toc33 and Toc34 independent of the ethylene signaling. Elevated levels of CTR1 also increased Toc75 protein abundance but did not affect Toc159 levels (fig. S8A).

### CTR1-mediated phosphorylation of Toc33/34 and functional phosphorylation sites

CTR1 has been previously characterized with EIN2 as its sole known phosphorylation substrate (15, 16). To investigate whether CTR1 also phosphorylates Toc33 and Toc34, we conducted an in vitro kinase assay using  $^{32}\text{P}[\gamma\text{ATP}]$  with *Escherichia coli*-purified CTR1 kinase, Toc33, and Toc34 proteins lacking their transmembrane domain (Toc33/34- $\Delta\text{TM}$ ) (Fig. 3A). In the presence of active CTR1 kinase (lacking the N terminus; CTR1-KD) but not its inactive form (CTR1-KD<sup>D694E</sup>) (26), both Toc33 and Toc34 were phosphorylated, confirming direct phosphorylation by CTR1 (Fig. 3B and fig. S8B). In vivo analysis using Phos-tag gel electrophoresis, which distinguishes phosphorylated proteins by retarding their migration, revealed that increased levels of Myc-CTR1 enhanced both the phosphorylation and

abundance of GFP-Toc33 and GFP-Toc34. This suggests that CTR1-mediated phosphorylation enhances the stability of both Toc33 and Toc34 (Fig. 3C and fig. S8C). This phosphorylation occurred independent of ETR1 and EIN2 (Fig. 3, D and E), indicating that CTR1 remains catalytically active in their absence and that CTR1 phosphorylates Toc33/34 outside the canonical ethylene signaling. Moreover, CTR1 did not phosphorylate other TOC proteins, such as Toc64, Toc75, and Toc159, highlighting its specificity for Toc33 and Toc34 within the TOC complex (fig. S8D).

To identify specific phosphorylation sites on Toc33, we performed mass spectrometry on samples from *Arabidopsis* protoplasts expressing Toc33 with or without CTR1. Our analysis identified seven phosphosites present exclusively in the presence of CTR1: the previously reported S181 site (10) and six newly identified sites, T173, S258, S260, Y276, T292, and S293 (Fig. 3F, fig. S9, and table S1). Among these sites, S258 and S260 were most frequently detected (table S1). Notably, previous genetic studies suggested that S181 may not be biologically important for Toc33 function (12, 13). To determine whether CTR1 phosphorylates these sites, we mutated S258, S260, and S181 to nonphosphorylatable alanine (A). The S181A mutation did not prevent CTR1 from phosphorylating Toc33 (fig. S10). Similarly, the S258A mutation permitted phosphorylation but led to reduced levels compared to WT Toc33. Notably, the S260A mutation completely abolished phosphorylation, establishing S260 as the critical phosphorylation site (Fig. 3G). The reduced phosphorylation of Toc33-S258A suggests that S258 plays an indirect role in the process. While this residue may not be directly phosphorylated, it may promote the proper recognition motif around S260, enabling optimal access for CTR1.

### The effect of CTR1-mediated phosphorylation on Toc33 ubiquitination and degradation

The CHLORAD pathway mediates Toc33 degradation through ubiquitination (4, 6). To investigate whether CTR1-mediated phosphorylation

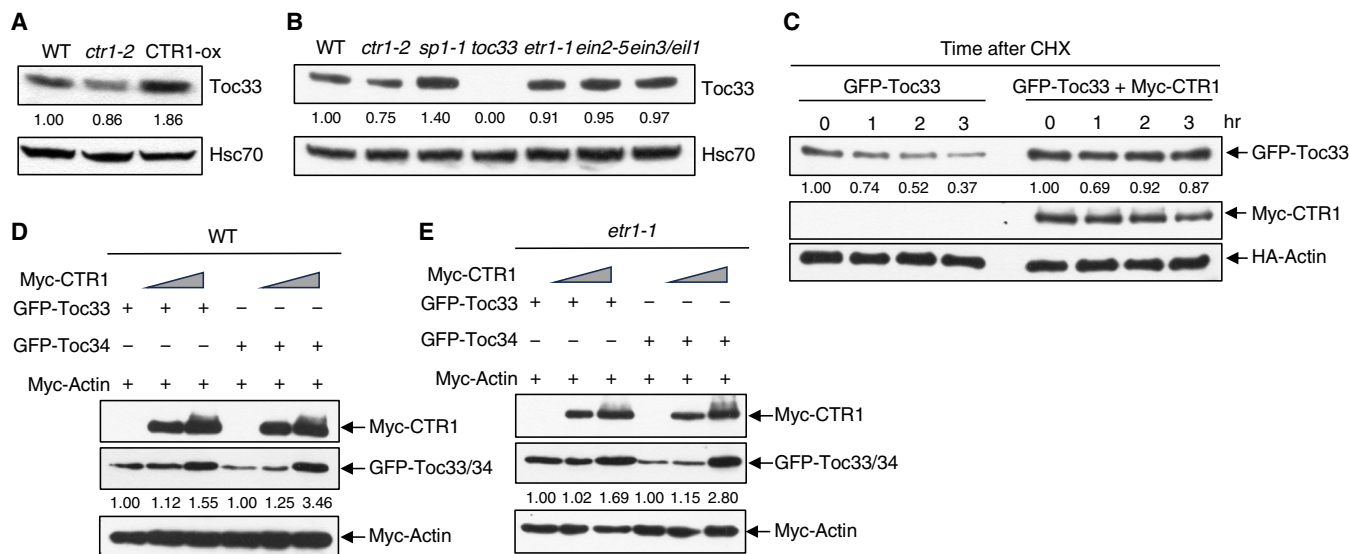


**Fig. 2. CTR1 positively regulates Toc33/34 independently of the ethylene signaling.** (A and B) Steady-state levels of Toc33 protein in 5-day-old seedlings: (A) WT, *ctr1-2*, and CTR1 overexpression (CTR1-ox) lines; and (B) WT, *ctr1-2*, *sp1-1*, *etr1-1*, *ein2-5*, and *ein3/eil1* mutants. (C) Stability of GFP-Toc33 protein with or without coexpression of Myc-CTR1 in *Arabidopsis* protoplasts. Cycloheximide (CHX; 500  $\mu\text{M}$ ) was used to block protein synthesis. (D and E) GFP-Toc33 protein levels increase with escalating Myc-CTR1 expression in protoplasts from (D) WT and (E) *etr1-1* plants. Protoplasts were cotransfected with a constant amount of GFP-Toc33 or GFP-Toc34 plasmids, alongside increasing amounts of CTR1. Myc-Actin was used as a transfection control.

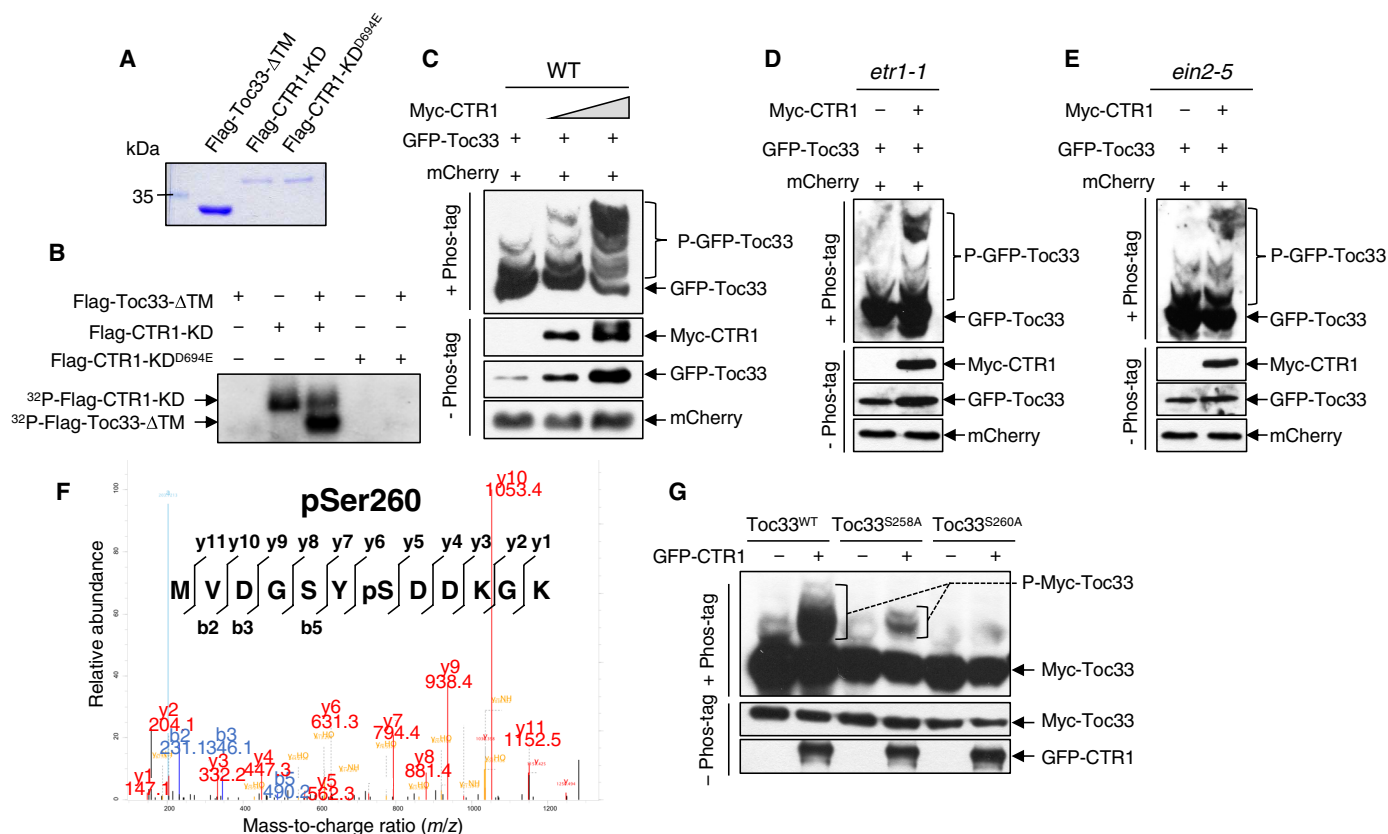


**Fig. 3. CTR1 phosphorylates Toc33 at Ser260.** (A) Purified protein for in vitro kinase assay. Flag-Toc33 lacking the transmembrane domain ( $\Delta$ TM), Flag-CTR1 kinase domain (KD), and the inactive Flag-CTR1 kinase domain mutant (Flag-CTR1-KD<sup>D694E</sup>) were purified from *E. coli*. (B) In vitro kinase assay using <sup>32</sup>P[ $\gamma$ ATP] radiolabeling. (C to E) GFP-Toc33 phosphorylation and abundance correspond to increasing Myc-CTR1 coexpression in protoplasts from (C) WT, (D) *etr1-1*, and (E) *ein2-5*. Protein samples were separated by SDS-PAGE with and without Phos-tag. (F) A phosphopeptide spectrum from tandem mass spectrometry (MS/MS) identifying Ser260 as a Toc33 phosphorylation site by CTR1. The mass shift between y5 and y6 (69 Da) confirms S260 phosphorylation (Ser mass 87 Da + phosphate 80 Da – neutral loss H<sub>3</sub>PO<sub>4</sub> 98 Da = 69 Da). (G) Phosphorylation of Myc-Toc33-WT, Myc-Toc33-S258A, or Myc-Toc33-S260A mutant proteins by GFP-CTR1 in *Arabidopsis* protoplasts, analyzed via SDS-PAGE with and without Phos-tag.

stabilizes Toc33 by suppressing this pathway, we examined how CTR1 affects Toc33 ubiquitination by the SP1 E3 ligase, a key component of the CHLORAD. To this end, we expressed Toc33 in *Arabidopsis* protoplasts either alone or together with CTR1 (Fig. 4A). To enrich ubiquitinated proteins, protoplasts were treated with a potent proteasome inhibitor bortezomib (Btz), which prevents the degradation of ubiquitinated proteins. After isolating GFP-tagged Toc33 using GFP-trap, we detected ubiquitinated GFP-Toc33 using an anti-ubiquitin antibody. While GFP-Toc33 levels remained constant, the amount of ubiquitinated GFP-Toc33 decreased substantially when coexpressed with CTR1, suggesting that CTR1 stabilizes Toc33 by inhibiting its ubiquitination (Fig. 4A). To further investigate the relationship between phosphorylation and ubiquitination, we compared the ubiquitination level of the Toc33-WT with a nonphosphorylatable Toc33-S260A variant (Fig. 4B). Following the same Btz treatment and GFP-tag enrichment steps, the Toc33-S260A variant exhibited higher levels of ubiquitination, indicating that phosphorylation negatively regulates Toc33 ubiquitination (Fig. 4B).

To confirm the regulatory role of S260 phosphorylation in SP1-mediated degradation, we compared the stability of Toc33-WT, nonphosphorylatable Toc33-S260A, and phospho-mimetic Toc33-S260D in the presence of increasing SP1 levels (Fig. 4C). Immunoblot analysis

revealed that while Toc33-WT showed gradual degradation with increasing SP1, Toc33-S260A degraded more rapidly. In contrast, Toc33-S260D remained stable even at high SP1 levels, suggesting that phosphorylation at S260 protects Toc33 from SP1-mediated degradation. Cycloheximide treatment further confirmed these findings, demonstrating that phospho-mimetic Toc33-S260D degrades more slowly than Toc33-WT (Fig. 4D).

### The biological relevance of Toc33-S260 phosphorylation in chloroplast biogenesis

To determine the functional impact of Toc33-S260 phosphorylation in planta, we generated stable transgenic lines expressing either the WT version of GFP-Toc33 or the nonphosphorylatable GFP-Toc33-S260A to complement the *toc33* null mutant. Phenotypic analysis of 4-day-old seedlings, when endogenous Toc33 expression is highest during early development (3) (fig. S11), showed that GFP-Toc33 effectively rescued the *toc33* mutant phenotype, whereas GFP-Toc33-S260A did not (Fig. 5A). The *GFP-Toc33/toc33* lines displayed chlorophyll levels similar to WT, whereas the *GFP-Toc33-S260A/toc33* lines had chlorophyll levels comparable to the *toc33* mutant (Fig. 5B). Quantification of *GFP-Toc33* transcript levels across all lines revealed that transcript levels were consistent, ruling out variations in

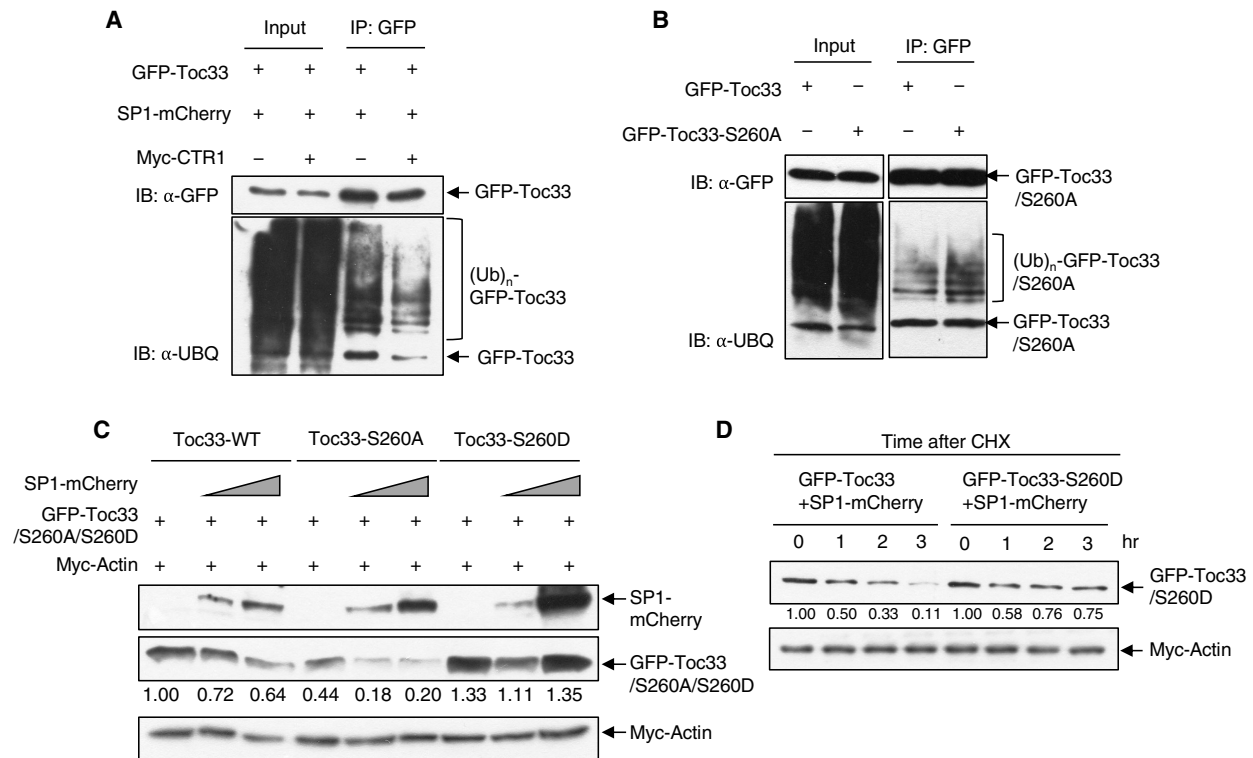


**Fig. 4. CTR1-mediated phosphorylation at Ser260 inhibits SP1-mediated ubiquitination and degradation of Toc33.** (A) Ubiquitination level of GFP-Toc33 under SP1-mCherry coexpression with or without Myc-CTR1 coexpression. (B) Ubiquitination level of GFP-Toc33 or GFP-Toc33-S260A. (A and B) *Arabidopsis* protoplasts were treated with 50  $\mu$ M bortezomib (Btz) for 2 hours before cell lysis and immunoprecipitation using GFP-trap. Proteins were immunoblotted with either anti-GFP or anti-ubiquitin (UBQ) antibodies. (C) SP1-mediated degradation of different Toc33 variants. The Toc33-WT, nonphosphorylatable Toc33 (Toc33-S260A), or the phospho-mimetic Toc33 (Toc33-S260D) were coexpressed with increased SP1 protein. The protein steady-state levels were detected. Myc-Actin was used as a transfection control. (D) The protein stability assay of GFP-Toc33 and GFP-Toc33-S260D in *Arabidopsis* protoplast. Cycloheximide (CHX; 500  $\mu$ M) was used to block protein synthesis. hr, hours.

gene expression due to T-DNA insertion sites as a factor (Fig. 5C). This confirms that the phenotypic differences were attributable to the reduced protein stability of the Toc33-S260A variant (Fig. 5D), rather than differences in transcript levels.

Toc33 is essential for accumulating photosynthetic proteins and the functionality of the photosynthetic apparatus (27). To assess the effect of the Toc33-S260A mutation on key photosynthetic components, we quantified both nuclear-encoded [light-harvesting chlorophyll B-binding 2 (Lhcb2) and photosystem I subunit H (PsaH)] and chloroplast-encoded [photosystem II reaction center protein A (PsbA) and Rubisco large subunit (RbcL)] proteins, which are markedly reduced in the *toc33* mutant (Fig. 5E). In *GFP-Toc33/toc33* lines, the levels of these proteins were effectively restored to near WT levels. By contrast, *GFP-Toc33-S260A* lines showed a pronounced deficiency in rescuing the nuclear-encoded Lhcb2 and PsaH, while modestly recovering the chloroplast-encoded PsbA and RbcL (Fig. 5E). These results demonstrate the importance of S260 phosphorylation for importing and maintaining photosynthetic protein abundance, especially nuclear-imported proteins (Fig. 5E).

To evaluate the impact of Toc33-S260 phosphorylation on chloroplast protein import, we measured the import rate of the <sup>35</sup>S-labeled Rubisco small subunit (RbcS) precursor, a nuclear-encoded chloroplast preprotein, into isolated chloroplasts from WT, *toc33*, *GFP-Toc33/toc33*, and *GFP-Toc33-S260A/toc33* lines. Import efficiency was assessed by the cleavage of the transit peptide and accumulation of the

mature RbcS protein. Chloroplasts from the *GFP-Toc33/toc33* displayed an import rate comparable to WT, whereas *GFP-Toc33-S260A/toc33* chloroplasts showed a considerably reduced import rate similar to the *toc33* mutant (Fig. 5, F and G).

*Toc33* is highly expressed in early seedling development, and the defective chloroplast ultrastructure observed in the cotyledons of the *ppi1* mutant indicates its importance in chloroplast biogenesis (3). Transmission electron microscope (TEM) of chloroplasts from WT, *toc33*, and *GFP-Toc33/toc33*, and *GFP-Toc33-S260A/toc33* lines revealed that *GFP-Toc33* fully restored chloroplast structure in *toc33*, including chloroplast size and the number of thylakoid layers (Fig. 5, H to J). In contrast, *GFP-Toc33-S260A* failed to restore normal chloroplast ultrastructure, mimicking the phenotype of the *toc33* mutant (Fig. 5, H to J). These results highlight the importance of Toc33-S260 phosphorylation by CTR1 for chloroplast biogenesis and structural integrity (Fig. 5H).

## DISCUSSION

This work uncovers an ethylene-independent role of CTR1 in regulating TOC protein stability and chloroplast biogenesis through phosphorylation. Traditionally known for its function as a negative regulator in the ethylene signaling at the ER, CTR1 has now been shown to extend its role to other cellular compartments, including the nucleus and chloroplast (20, 22). Following cytoplasmic translation,

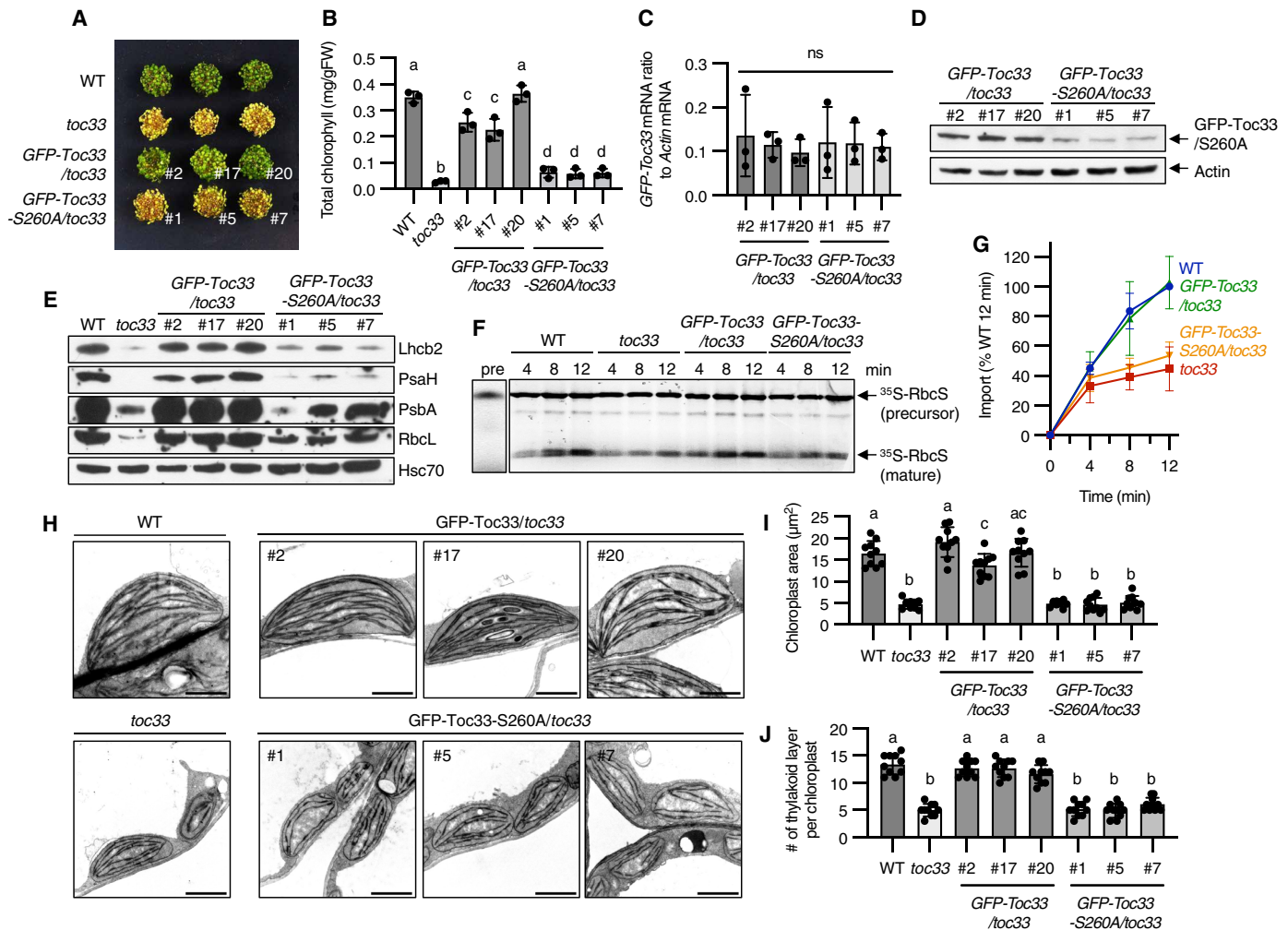


**Fig. 5. CTR1-mediated phosphorylation of Toc33 at Ser260 is essential for chloroplast protein import and chloroplast biogenesis.** (A) Representative phenotypes of 4-day-old seedlings from WT, *toc33* mutants, and three independent transgenic lines expressing either GFP-Toc33 or the phosphorylation-deficient GFP-Toc33-S260A variant in the *toc33* background. (B) Quantification of chlorophyll content in WT, *toc33*, and the six transgenic lines expressing either GFP-Toc33 or GFP-Toc33-S260A. Three biological replicates were conducted. (C) Relative mRNA levels of *GFP-Toc33* in the six transgenic lines, measured by qRT-PCR. Three biological replicates were conducted. One-way analysis of variance (ANOVA) shows no significant differences among the six lines. (D) Protein levels of GFP-Toc33 in the six transgenic lines, detected by immunoblotting. (E) Immunoblot analysis of selected chloroplast proteins in WT, *toc33*, and the six transgenic lines. Lhcb2 and PsaH (nuclear-encoded) and PsbA and RbcL (chloroplast-encoded) were detected, with Hsc70 serving as the loading control. (F) Chloroplast protein import assay using isolated chloroplasts from WT, *toc33*, *GFP-Toc33/toc33*, and *GFP-Toc33-S260A/toc33*. The <sup>35</sup>S-labeled Rubisco small subunit (RbcS) precursor protein was used as an import substrate, and mature RbcS import was assessed. (G) Quantification of <sup>35</sup>S-labeled mature RbcS import efficiency from two biological replicates. (H) Transmission electron microscopy images showing chloroplast ultrastructure of 4-day-old WT, *toc33*, and the six complementation lines. Scale bars, 2  $\mu\text{m}$ . (I and J) Quantification of (I) chloroplast area and (J) number of thylakoid layers in chloroplasts from 4-day-old WT, *toc33*, and the complementation lines. Ten chloroplasts were measured per line. [(B), (I), and (J)] A one-way ANOVA indicated significant differences among the lines. *t*-tests were performed to compare the different groups. A different letter display was used to identify groups that show statistical differences ( $P < 0.05$ ).

CTR1 is directed to distinct destinations, such as the ER and chloroplasts, likely mediated by interacting partners. At the chloroplast membrane, CTR1 functions independently of core ethylene signaling components EIN2 and ETR1, phosphorylating and stabilizing Toc33 and Toc34 to regulate the import of nuclear-encoded chloroplast proteins (Fig. 6). Since ethylene plays a profound role in chloroplast function and photosynthesis (28), the constitutive ethylene response in *ctr1* mutants could mask chloroplast phenotypes regulated by the TOC complex. To observe CTR1-specific effects, we examined the ethylene-insensitive *ctr1ein2* double-null mutant. Unexpectedly, *ctr1ein2* did not exhibit noticeable changes in chlorophyll contents or

chloroplast ultrastructure compared to the *ein2* single mutant (fig. S12A to C). This lack of distinct phenotypes could be attributed to several possibilities. Unlike the *toc33* null mutant, which produces no functional Toc33 protein, the residual Toc33 protein in *ctr1-2*, though reduced, may be sufficient to maintain essential chloroplast import. In addition, functional redundancy among Toc33-phosphorylating kinases may compensate for the loss of CTR1, thereby maintaining TOC complex function. CTR1 is a mitogen-activated protein kinase kinase kinase (MAPKKK), and the *Arabidopsis* genome contains over 80 such kinases (28). Within this extensive family, CTR1 is classified as an RAF-like MAPKKK, part of a subgroup that consists of 48 kinases

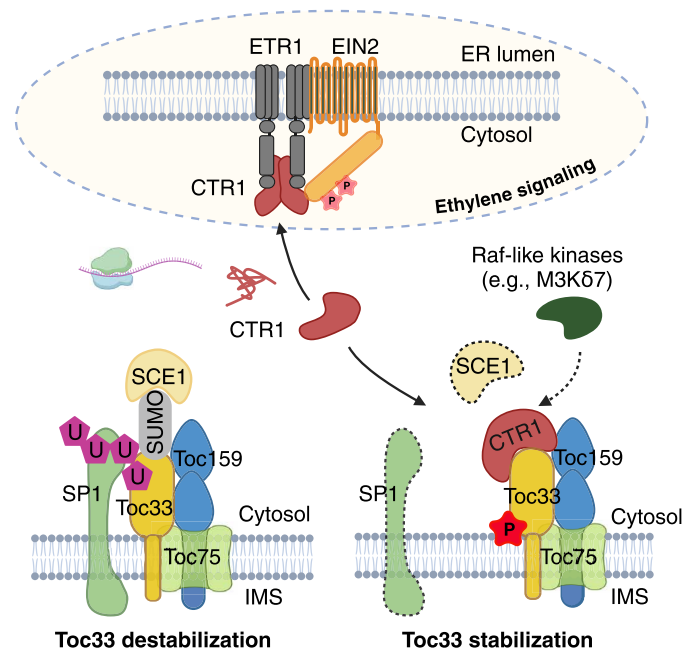


**Fig. 6. Model for ethylene-independent CTR1 functions in TOC complex regulation.** In ethylene signaling, CTR1 acts as a negative regulator by phosphorylating EIN2 at the ER, suppressing ethylene responses during normal growth conditions. Independent of this role, CTR1 also localizes to the chloroplast outer membrane, where it phosphorylates and stabilizes TOC translocon components such as Toc33 and Toc34. This phosphorylation prevents Toc33 degradation by the E3 ligase SP1, facilitating the import of nuclear-encoded preproteins into chloroplasts and maintaining the photosynthetic machinery. CTR1's role in regulating TOC protein stability may extend beyond SP1 inhibition, possibly involving additional degradation pathways, such as SUMOylation-mediated degradation via SCE1. By stabilizing Toc33 against multiple degradation pathways, CTR1 may ensure proper chloroplast biogenesis and function during the transition from plastids to mature chloroplasts. In addition, functional redundancy with other MAPKKs, such as M3K87, compensates for CTR1 loss in TOC regulation, warranting continued chloroplast development and regulation. This redundancy highlights the robust nature of the regulatory network governing chloroplast protein import. This cartoon was created in BioRender. Chien (2024), BioRender.com/d73k509.

divided into three groups (A, B, and C). CTR1 specifically belongs to the B3 subgroup, which includes six closely related B3 kinases (fig. S13A) (28). Phos-tag gel analysis revealed that while SIS8 (At1g73660), EDR1 (At1g08720), RAF6 (At4g24480), and MKD1 (At5g11850) do not phosphorylate Toc33, M3K87 (At1g18160) does phosphorylate Toc33 (fig. S13B). Similarly, RAF6, MKD1, and M3K87 phosphorylate Toc34 (fig. S13C). These results suggest that Toc33 and Toc34 phosphorylation involves multiple B3 RAF kinases, potentially including additional unidentified MAPKKs, highlighting the intricate regulation of the TOC translocon in chloroplast biology. The crucial impact of Toc33-S260 in maintaining both photosynthetic protein levels and structural integrity suggests that S260 could be a primary target site for RAF-like kinases. While these kinases show potential functional overlap in TOC regulation, CTR1 appears to be a key player in regulating Toc33 stability, as *ctr1-2* null mutants showed markedly reduced Toc33 abundance even when other RAF-like kinases remained functional (Fig. 2, A and B, and fig. S7). Further genetic studies using higher-order mutants lacking both CTR1 and other RAF-like kinases will be needed to directly demonstrate

their *in vivo* roles in TOC regulation and broader influence on plant biology.

The interplay between different PTMs, including ubiquitination, SUMOylation, and phosphorylation, regulates the stability of the Toc33 protein (4–7, 29). Key players in these processes include E3 ligases SP1, SPL1, and SPL2 (4, 5), SUMO-conjugating enzyme SCE1 (7), the kinases CTR1, and potentially M3K87 identified in this study (Fig. 6). The PTMs regulated by these proteins form a complex regulation network that fine-tunes Toc33 stability during different developmental stages and stress responses. Ubiquitination and SUMOylation negatively affect Toc33 protein stability (4, 6, 7), while phosphorylation acts as a positive regulator. Recent ubiquitinome profiling identified a ubiquitination site at Toc34-K248, which is conserved at Toc33-K246 (30), near the phosphorylation site S260 identified in our study. This proximity suggests potential cross-talk between ubiquitination and phosphorylation in regulating Toc33 stability. In this study, we demonstrated that phosphorylation at S260 down-regulates Toc33 ubiquitination (Fig. 4), possibly by inducing conformational changes that hinder ubiquitin-conjugating enzyme binding. Notably, while phosphorylation of Toc33 at S260 by CTR1 inhibits SP1-mediated ubiquitination, CTR1 still phosphorylated and stabilized Toc33/34 in the *sp1* mutant (fig. S14, A and B). This observation suggests the existence of additional E3 ligases that regulate Toc33/34 ubiquitination, potentially antagonized by CTR1. Future studies in identifying additional E3 ligases or additional PTM-reversing components, such as phosphatases, deubiquitinating enzymes, and SUMO proteases, will be crucial for elucidating the full scope of the regulatory network governing Toc33 stability via the PTMs.

In this study, we identify a phosphorylation site in Toc33 and demonstrate the involvement of CTR1 in this process. We show that this PTM is essential for chloroplast biogenesis by modulating Toc33 protein stability. Notably, *Toc33-S260A* lines barely rescued the chloroplast ultrastructure defects in *toc33*, yet they partially restored nuclear-encoded chloroplast gene expression, displaying a mild *genome uncoupled (gun)* mutant phenotype (Fig. 5, E and H) (31). This finding suggests a potential link between CTR1-mediated TOC regulation and retrograde signaling, though this relationship requires further investigation. Future research should also investigate the broader effects of RAF-like kinases on TOC complex formation and their roles in chloroplast proteome dynamics, development, and stress responses. Understanding these processes could guide strategies to enhance chloroplast function and, ultimately, increase crop productivity.

## MATERIALS AND METHODS

### Plant material and growth conditions

All *Arabidopsis thaliana* plants used in this study are of the Col-0 ecotype. Most plants were grown in a continuous light growth chamber at  $22^{\circ} \pm 2^{\circ}\text{C}$ , except for those used for protoplast transfection, which are grown in a 12-hour light/12-hour dark chamber. The plants used for protein-localization imaging and immunoblot were 5-day-old seedlings grown on  $\frac{1}{2}$  Murashige and Skoog (MS) basal medium supplemented with 0.8% plant agar (pH 5.7). The mutants used in this study, *ein2-5* (32), *ctr1-2* (14), *sp1-1* (4), *etr1-1* (33), *ein3/eil1* (34), *ctr1-1* (14), *ctr1ein2W308\** (35), and *ein2W308\** (35), were previously described. The *toc33* (SALK\_205203C) was obtained from Arabidopsis Biological Resource Center (ABRC).

The primers used for genotyping *toc33* (SALK\_205203C) are listed in table S3.

### Stable transgenic plant generation

All stable transgenic *Arabidopsis* plants were generated using the floral dipping method. All transgenic plants used in this study are homozygous T3 lines with single gene insertion identified by the segregation of antibiotic resistance followed by the confirmation of protein expression via immunoblot analyses.

All molecular cloning was performed with the Gateway (Invitrogen) or infusion cloning (Takara Bio USA) strategies unless otherwise specified. The construct used to create GFP-CTR1/*ctr1-2* and GFP-CTR1/*ein2-5* is described previously (20). The construct for expressing mCherry-Toc33 was generated by cloning both the mCherry fragment and the coding sequence of *Toc33* into the pENTR plasmid. The mCherry-Toc33 fragment was then transferred to the destination vector pEarlyGate 100 for gene expression in plants driven by a 35S promoter.

The pENTR223-Toc33 plasmid was obtained from ABRC (stock number: G83552). The *Toc33* fragment was transferred to the pSITE2CA destination vector by Gateway cloning for GFP-Toc33 expression. The S260A mutation was introduced by polymerase chain reaction (PCR)-based mutagenesis of the entire pENTR223-Toc33 plasmid, followed by infusion cloning. The pENTR223-Toc33-S260A was then transferred to the pSITE2CA destination vector for GFP-Toc33-S260A expression.

### Bimolecular fluorescence complementation

The constructs used to express nYFP-CTR1 were described previously (22). The coding sequences of *Toc33*, *Toc34*, *Toc159*, and *JASSY* are cloned into pENTR plasmids and then transferred to pCL113 vector for cYFP-Toc33/34/159 and pBAT-TL-cYFP for *JASSY*-cYFP protein expression.

For BiFC performed in *Arabidopsis* protoplasts, plasmids expressing nYFP-CTR1 and cYFP-Toc33/34/159, *JASSY*-cYFP were cotransfected into *Arabidopsis* protoplasts. Imaging was performed 16 hours after transfection. For BiFC performed in *Nicotiana benthamiana*, the plasmids that expressed nYFP-CTR1 and cYFP-Toc33/34/159, *JASSY*-cYFP were transformed into *Agrobacterium* GV3101. Expression of nYFP-CTR1 and cYFP-Toc33/34/159, *JASSY*-cYFP in *N. benthamiana* was achieved using an Agro-infiltration method, and imaging was performed 3 days after transfection.

### Coimmunoprecipitation

The construct used to express GFP-CTR1 has been previously described (20). The construct pUC19-GFP was used for GFP expression. To create the Myc-Toc33 construct, the *Toc33* fragment was transferred from pENTR223-Toc33 to the pEG203 destination vector. Protoplasts were transfected to express Myc-Toc33 along with either GFP-CTR1 or GFP. Following transfection, the protoplasts were lysed with radioimmunoprecipitation assay (RIPA) buffer supplemented with 1× Halt protease inhibitor cocktail (Thermo Fisher Scientific) for 20 min in a cold room and then diluted twofold with washing buffer [10 mM tris-HCl (pH 7.5), 150 mM NaCl, and 0.5 mM EDTA]. GFP-tagged proteins were pulled down using GFP-trap magnetic agarose (ChromoTek) for 1 hour and washed three times with washing buffer. The proteins were eluted by boiling in 2× Laemmli SDS sample buffer and Myc-Toc33 protein was detected via immunoblotting.

### Confocal microscopy

All imaging was performed with a laser-scanning confocal microscope (Zeiss LSM880 upright). Five-day-old transgenic seedlings were used to observe GFP-CTR1 and GFP localization, and GFP-CTR1 and mCherry-Toc33 colocalization.

### Protoplast transient expression

The protoplast transfection method was described previously (36). For transfection with multiple plasmids, different plasmids were mixed to a total amount of 10 to 15 μg per reaction, with an empty vector used to balance the plasmid amount. For example, to observe GFP-Toc33 abundance regulation with an increasing amount of Myc-CTR1, the plasmid compositions of the three reactions were set up as follows: (i) 5 μg of the plasmid expressing GFP-Toc33, 5 μg of the empty vector, and 2 μg of the plasmid expressing Myc-Actin; (ii) 5 μg of the plasmid expressing GFP-Toc33, 1 μg of the plasmid expressing Myc-CTR1, 4 μg of the empty vector, and 2 μg of the plasmid expressing Myc-Actin; and (iii) 5 μg of the plasmid expressing GFP-Toc33, 5 μg of the plasmid expressing Myc-CTR1, and 2 μg of the plasmid expressing Myc-Actin.

The construct used for Myc-CTR1 expression was described previously (20). The construct for expressing GFP-Toc33 is described in the transgenic plant generation section. The constructs for expressing GFP-Toc34, GFP-Toc64, GFP-Toc75, and GFP-Toc159 were generated by cloning the coding sequences of *Toc34* (At5g05000), *Toc64* (At3g17970), *Toc75* (At3g46740), and *Toc159* (At4g02510) into pENTR plasmids. The resulting pENTR plasmids were then transferred to the pSITE2CA destination vector for GFP-tagged TOC expression. The plasmid for expressing Myc-Actin was generated by cloning the coding region of *ACT8* (At1g49240) into the pENTR plasmid, then transferred to the pEarlyGate 203 plasmid.

The constructs for S258A, S260A, and S260D mutations were created by PCR-based mutagenesis of the entire pENTR223-Toc33 plasmid, followed by the infusion cloning method. The Myc-Toc33/S258A/S260A constructs were cloned by transferring the *Toc33* fragments from the entry vector to the pEarlyGate 203 destination vector. The GFP-Toc33/S260D construct was cloned by transferring the *Toc33* fragments from the entry vector to the pSITE2CA destination vector.

### In vitro kinase assay

The gene fragments of *Toc33* and *Toc34*, with their transmembrane domains removed (*Toc33*<sup>1-258</sup> and *Toc34*<sup>1-260</sup>), and the CTR1 kinase domain (CTR1<sup>533-822</sup>) were amplified from *Arabidopsis* cDNA and cloned into the pFlag-MAC vector for *E. coli* protein expression. The inactive CTR1 kinase domain containing the D694E mutation was generated by PCR-based mutagenesis from the pFlag-MAC-CTR1-KD construct.

All proteins were expressed in BL21 (Rosetta) cells. The *E. coli* cells were grown using the Zymo Dual Media Set, following the manufacturer's protocol. The soluble fractions of total proteins were purified using GenScript Anti-DYKDDDDK G1 Affinity Resin (catalog no. L00432). A total of 10 ng of purified Flag-CTR1-KD or Flag-CTR1-KD<sup>D694E</sup> was incubated with 100 ng of Flag-Toc33/34-ΔTM in kinase reaction buffer [50 mM tris (pH 7.5), 10 mM MgCl<sub>2</sub>, 1× Roche Complete Protease Inhibitor mixture, and 1 μCi [<sup>32</sup>P] ATP] for 30 min at room temperature. After incubation, the reactions were terminated by boiling in 6× Laemmli SDS sample buffer for 3 min. Samples were subjected to SDS-polyacrylamide gel electrophoresis (PAGE), dried, and visualized by autoradiography.

### Phos-tag gel analysis

Preparation of Phos-tag polyacrylamide gels and subsequent immunoblotting were performed according to the manufacturer's instructions. The Phos-tag gel was prepared with 5 ml of 8% acrylamide containing 50  $\mu$ M Phos-tag (Wako) for the resolving gel and 4 ml of 4.5% acrylamide for the stacking gel. The protoplast samples in Laemmli SDS sample buffer were supplemented with 1 mM ZnCl<sub>2</sub> before loading into the Phos-tag gel. Electrophoresis was carried out for 4 hours at 100 V in a cold room. After electrophoresis, the gel was incubated in transfer buffer containing 0.2% (w/v) SDS and 10 mM EDTA for 10 min, repeated three times. The gel was then transferred to a nitrocellulose membrane at 20 V for 90 min using a semi-dry method. The following steps were performed as in a standard immunoblot.

### Protein stability assay

Sixteen hours after protoplast transfection, the protoplasts were treated with 500  $\mu$ M cycloheximide. Samples were collected over time, and the reactions were stopped by harvesting the protoplasts via centrifugation, followed by boiling in 2 $\times$  Laemmli SDS sample buffer. The protoplast samples were then analyzed by immunoblot.

### Protein ubiquitination detection

Sixteen hours post-transfection, protoplasts were treated with 50  $\mu$ M Btz a proteasome inhibitor, for 2 hours. Following treatment, the protoplasts were harvested by centrifugation and lysed using RIPA buffer supplemented with 1 $\times$  Halt protease inhibitor cocktail (Thermo Fisher Scientific) for 20 min in a cold room. The lysates were then diluted twofold with washing buffer [10 mM Tris-HCl (pH 7.5), 150 mM NaCl, and 0.5 mM EDTA]. GFP-tagged proteins were pulled down using GFP-trap magnetic agarose (ChromoTek) for 1 hour and subsequently washed three times with washing buffer. Proteins were eluted by boiling in 2 $\times$  Laemmli SDS sample buffer. Following elution, the proteins were separated by SDS-PAGE at a low voltage (80 V) until the dye front reached the bottom of the gel. Last, the proteins were transferred to a membrane and immunoblotted using either anti-GFP or anti-ubiquitin antibodies.

### Immunoblot analysis

For protein detection in seedlings, the seedlings were harvested, blotted dry, and ground into a fine powder before being resuspended in 2 $\times$  Laemmli SDS sample buffer. For protein detection in protoplast samples, the protoplasts were harvested by centrifugation and resuspended in 2 $\times$  Laemmli SDS sample buffer. The samples were boiled for 5 min and centrifuged to remove any debris before loading into the SDS-PAGE gel. After SDS-PAGE, the gel was transferred to a nitrocellulose membrane using the semi-dry method. The membrane was then blocked with 5% milk and incubated with the primary antibody solution in 3% milk. Signals were detected using SuperSignal West Pico or Femto Maximum Sensitivity Substrate (Thermo Fisher Scientific, catalog nos. 34580 and 34095), and band intensities were measured using ImageJ software. The relative abundance of protein was normalized to the band intensity of the loading control using ImageJ software.

### Antibodies used in this study

The CTR1 and Toc33 antibodies were purified from rabbit serum raised against purified Flag-CTR1-KD and His-Toc33- $\Delta$ TM, respectively. The production of the rabbit serum was carried out by Pacific Immunology. The construct for expressing His-Toc33- $\Delta$ TM was generated by first cloning the Toc33 fragment without the

transmembrane domain (Toc33<sup>1-258</sup>) into pENTR, then transferring it to the pDEST17 destination vector. The construct for expressing Flag-CTR1-KD was described in the "In vitro kinase assay" section. Both Flag-CTR1-KD and His-Toc33- $\Delta$ TM proteins were expressed in BL21 (Rosetta) cells. The soluble protein fractions were purified using Pierce Anti-DYKDDDDK Magnetic Agarose (catalog no. 2162708) and HisPur Cobalt Resin (catalog no. 89964), respectively. Two milligrams of purified Flag-CTR1-KD and His-Toc33- $\Delta$ TM proteins were separated by SDS-PAGE, and the targeted bands were excised and sent for rabbit immunization. Table S2 describes the commercially purchased antibodies used in this study and their respective dilution factors.

### LC-MS/MS analysis

To prepare samples for liquid chromatography–tandem mass spectrometry (LC-MS/MS), protoplasts were first transfected to express either GFP-Toc33 alone or both GFP-Toc33 and Myc-CTR1. The protoplast samples were harvested by centrifugation and dissolved in 300  $\mu$ l of 50 mM triethylammonium bicarbonate (TEAB) buffer. Protein concentration was measured using the bicinchoninic acid assay. A total of 500  $\mu$ g of protein was precipitated with 4 volumes of ice-cold acetone, and the precipitation was carried out at  $-20^{\circ}$ C for at least 4 hours. The precipitate was pelleted by centrifugation at full speed for 15 min at  $4^{\circ}$ C, and the protein pellet was dried for 1 to 2 min in a SpeedVac. For reduction and alkylation, the protein pellet was first resuspended in 50  $\mu$ l of 8.0 M urea and vortexed for 20 min or until the solution became homogenized. Dithiothreitol (DTT) was then added to a final concentration of 5 mM, and the reaction was incubated at  $37^{\circ}$ C for 30 min. Subsequently, iodoacetamide was added to the solution to a final concentration of 20 mM and incubated at room temperature in the dark for 30 min. An additional 8  $\mu$ l of 250 mM DTT was added to the solution and incubated at room temperature in the dark for 10 min. For trypsin digestion, 250  $\mu$ l of 50 mM TEAB and 20  $\mu$ g of trypsin were added, and the reaction was incubated overnight at  $37^{\circ}$ C. The samples were desalted using a Pierce C18 spin column (Thermo Fisher Scientific) and phosphoenriched using the Spin-Tip PolyMAC-Ti Phosphopeptide Enrichment Kit (Tymora) following the manufacturer's protocol. The samples were processed using the Orbitrap Fusion Lumos (Thermo Fisher Scientific). Raw MS/MS data were searched against the Uniprot *Arabidopsis* database using Maxquant software. Spectra of phosphopeptide were exported from Maxquant, and the mass/charge ratio value was enlarged for clearer view. All phosphorylation was confirmed by calculating the mass shift of the phospho-serine or phospho-threonine.

### Chlorophyll measurement

Chlorophyll measurement was performed using the acetone extraction method as previously described (37).

### RNA isolation and qRT-PCR

Total RNA was extracted using the RNeasy Plant Mini Kit (QIAGEN, catalog no. 74904) and reverse transcribed with the All-In-One 5X RT MasterMix (abm, catalog no. G592) according to the manufacturer's instructions. Quantitative reverse transcriptase PCR (RT-PCR) was performed using 2X SYBR Green Master Mix (Selleck, catalog no. B21203) on a Roche LightCycler 96 machine. Three biological replicates were conducted for each sample. The relative expression of the selected gene was normalized to *Actin 2*. The primers used for quantitative PCR are listed in table S3.

## Chloroplast isolation, protein import, and thermolysin treatment

The chloroplast isolation and protein import were performed using 8-day-old seedlings as described previously (38). The plasmid used for precursor protein in vitro transcription and translation was generated by cloning the coding sequence of the Rubisco small subunit (RbcS) gene into the multiple cloning sites of the pENTR vector, which was then transferred to the pDEST17 destination vector. The DNA fragment containing a T7 promoter and the RbcS gene was amplified and subsequently used for in vitro transcription and translation with the TnT Quick Coupled Transcription/Translation System (Promega) following the manufacturer's instructions. One microcurie of <sup>35</sup>S-Met was added to the reaction to label the protein. The chloroplast protein import reaction was performed as described previously (38). After the reaction, the samples were subjected to SDS-PAGE, dried, and visualized by autoradiography. Two biological replicates were performed, and the band intensity was quantified using ImageJ. The import percentage was calculated by normalizing the mature RbcS protein band intensity at a specific time point for each genotype to the band intensity at the 12-min time point for WT chloroplasts.

For thermolysin treatment, isolated chloroplasts were treated with 400 μM thermolysin (Sigma-Aldrich, P1512) for 30 min on a rotating wheel at 4°C. Afterward, the chloroplasts were harvested by centrifugation and boiled in 2× SDS sample buffer for immunoblot analysis.

## Transmission microscopy (TEM)

All samples used for TEM were 4-day-old seedlings grown on ½ MS basal medium supplemented with 0.8% plant agar (pH 5.7). The samples were fixed in 2.5% glutaraldehyde in 0.1 M cacodylate buffer overnight at 4°C. They were then rinsed three times with 0.1 M phosphate buffer (pH 7.4) before undergoing postfixation in 1% osmium tetroxide and 1.5% potassium ferrocyanide in 0.1 M phosphate buffer (pH 7.4). The samples were stained with 2% uranyl acetate before being dehydrated through a series of ethanol and acetonitrile washes. Afterward, the samples were embedded in Spurr's low-viscosity resin and sectioned into ultrathin slices (70 nm) using a Leica Ultracut S ultramicrotome and a diamond knife. All samples were examined using a Tecnai T12 Transmission Microscope. At least 10 chloroplasts from each sample were recorded, and representative chloroplasts were displayed. The chloroplast area was measured using ImageJ, and the number of thylakoid layers per chloroplast was counted manually.

## Graph display and statistics

All graphs and statistics in the study were created by Prism 10.

## Supplementary Materials

This PDF file includes:

Figs. S1 to S14

Tables S1 to S3

## REFERENCES AND NOTES

- C. Andrés, B. Agne, F. Kessler, The TOC complex: Preprotein gateway to the chloroplast. *Biochim. Biophys. Acta Mol. Cell Res.* **1803**, 715–723 (2010).
- E. Demarsy, A. M. Lakshmanan, F. Kessler, Border control: Selectivity of chloroplast protein import and regulation at the TOC-complex. *Front. Plant Sci.* **5**, 1–10 (2014).
- P. Jarvis, L.-J. Chen, H. Li, C. A. Peto, C. Fankhauser, J. Chory, An *Arabidopsis* mutant defective in the plastid general protein import apparatus. *Science* **282**, 100–103 (1998).
- Q. Ling, W. Huang, A. Baldwin, P. Jarvis, Chloroplast biogenesis is regulated by direct action of the ubiquitin-proteasome system. *Science* **338**, 655–659 (2012).
- S. M. Ali, N. Li, Z. Soufi, J. Yao, E. Johnsson, Q. Ling, R. P. Jarvis, Multiple ubiquitin E3 ligase genes antagonistically regulate chloroplast-associated protein degradation. *Curr. Biol.* **33**, 1138–1146.e5 (2023).
- Q. Ling, W. Broad, R. Trösch, M. Töpel, T. D. Sert, P. Lymperopoulos, A. Baldwin, R. P. Jarvis, Ubiquitin-dependent chloroplast-associated protein degradation in plants. *Science* **363**, eaav4467 (2019).
- S. J. Watson, N. Li, Y. Ye, F. Wu, Q. Ling, R. P. Jarvis, Crosstalk between the chloroplast protein import and SUMO systems revealed through genetic and molecular investigation in *Arabidopsis*. *eLife* **10**, e60960 (2021).
- S. Accossato, F. Kessler, V. Shanmugabalaaji, SUMOylation contributes to proteostasis of the chloroplast protein import receptor TOC159 during early development. *eLife* **9**, e60968 (2020).
- M. Oreb, A. Höfle, O. Mirus, E. Schleiff, Phosphorylation regulates the assembly of chloroplast import machinery. *J. Exp. Bot.* **59**, 2309–2316 (2008).
- M. Jelic, J. Soll, E. Schleiff, Two Toc34 homologues with different properties. *Biochemistry* **42**, 5906–5916 (2003).
- N. Sveshnikova, J. Soll, E. Schleiff, Toc34 is a preprotein receptor regulated by GTP and phosphorylation. *Proc. Natl. Acad. Sci. U.S.A.* **97**, 4973–4978 (2000).
- M. Oreb, M. Zoryan, A. Vojta, U. G. Maier, L. A. Eichacker, E. Schleiff, Phospho-mimicry mutant of atToc33 affects early development of *Arabidopsis thaliana*. *FEBS Lett.* **581**, 5945–5951 (2007).
- H. Aronsson, J. Combe, R. Patel, P. Jarvis, In vivo assessment of the significance of phosphorylation of the *Arabidopsis* chloroplast protein import receptor, atToc33. *FEBS Lett.* **580**, 649–655 (2006).
- J. J. Kieber, M. Rothenberg, G. Roman, K. A. Feldmann, J. R. Ecker, CTR1, a negative regulator of the ethylene response pathway in *Arabidopsis*, encodes a member of the Raf family of protein kinases. *Cell* **72**, 427–441 (1993).
- C. Ju, G. M. Yoon, J. M. Shemansky, D. Y. Lin, Z. I. Ying, J. Chang, W. M. Garrett, M. Kessenbrock, G. Groth, M. L. Tucker, B. Cooper, J. J. Kieber, C. Chang, CTR1 phosphorylates the central regulator EIN2 to control ethylene hormone signaling from the ER membrane to the nucleus in *Arabidopsis*. *Proc. Natl. Acad. Sci. U.S.A.* **109**, 19486–19491 (2012).
- H. Qiao, Z. Shen, S. C. Huang, R. J. Schmitz, M. A. Urich, S. P. Briggs, J. R. Ecker, Processing and subcellular trafficking of ER-tethered EIN2 control response to ethylene gas. *Science* **338**, 390–393 (2012).
- X. Wen, C. Zhang, Y. Ji, Q. Zhao, W. He, F. An, L. Jiang, H. Guo, Activation of ethylene signaling is mediated by nuclear translocation of the cleaved EIN2 carboxyl terminus. *Cell Res.* **22**, 1613–1616 (2012).
- Z. Gao, Y. F. Chen, M. D. Randlett, X. C. Zhao, J. L. Findell, J. J. Kieber, G. E. Schaller, Localization of the Raf-like kinase CTR1 to the endoplasmic reticulum of *Arabidopsis* through participation in ethylene receptor signaling complexes. *J. Biol. Chem.* **278**, 34725–34732 (2003).
- K. L. Clark, P. B. Larsen, X. Wang, C. Chang, Association of the *Arabidopsis* CTR1 Raf-like kinase with the ETR1 and ERS ethylene receptors. *Proc. Natl. Acad. Sci. U.S.A.* **95**, 5401–5406 (1998).
- H. L. Park, D. H. Seo, H. Y. Lee, A. Bakshi, C. Park, Y.-C. Chien, J. J. Kieber, B. M. Binder, G. M. Yoon, Ethylene-triggered subcellular trafficking of CTR1 enhances the response to ethylene gas. *Nat. Commun.* **14**, 365 (2023).
- Y. C. Chien, G. M. Yoon, Subcellular dynamics of ethylene signaling drive plant plasticity to growth and stress: Spatiotemporal control of ethylene signaling in *Arabidopsis*. *Bioessays* **46**, e2400043 (2024).
- Y. Chien, A. Reyes, H. L. Park, S. Xu, G. M. Yoon, Uncovering the proximal proteome of CTR1 through TurboID-mediated proximity labeling. *Proteomics* **24**, e2300212 (2024).
- Q. Li, H. Fu, X. Yu, X. Wen, H. Guo, Y. Guo, J. Li, The SALT OVERLY SENSITIVE 2–CONSTITUTIVE TRIPLE RESPONSE1 module coordinates plant growth and salt tolerance in *Arabidopsis*. *J. Exp. Bot.* **75**, 391–404 (2024).
- E. M. Terrell, D. K. Morrison, Ras-mediated activation of the Raf family kinases. *Cold Spring Harb. Perspect. Med.* **9**, a033746 (2019).
- L. Guan, N. Denkert, A. Eisa, M. Lehmann, I. Sjuts, A. Weiberg, J. Soll, M. Meinecke, S. Schwenkert, JASSY, a chloroplast outer membrane protein required for jasmonate biosynthesis. *Proc. Natl. Acad. Sci. U.S.A.* **116**, 10568–10575 (2019).
- Y. Huang, H. Li, C. E. Hutchison, J. Laskey, J. J. Kieber, Biochemical and functional analysis of CTR1, a protein kinase that negatively regulates ethylene signaling in *Arabidopsis*. *Plant J.* **33**, 221–233 (2003).
- S. Kubis, A. Baldwin, R. Patel, A. Razzaq, P. Dupree, K. Lilley, J. Kurth, D. Leister, P. Jarvis, The *Arabidopsis* ppi1 mutant is specifically defective in the expression, chloroplast import, and accumulation of photosynthetic proteins. *Plant Cell* **15**, 1859–1871 (2003).
- MAPK Group, Mitogen-activated protein kinase cascades in plants: A new nomenclature. *Trends Plant Sci.* **7**, 301–308 (2002).
- C. Wan, H. Zhang, H. Cheng, R. Sowden, W. Cai, P. Jarvis, Q. Ling, Selective autophagy regulates chloroplast protein import and promotes plant stress tolerance. *EMBO J.* **42**, e112534 (2023).

30. Y. Sun, Z. Yao, Y. Ye, J. Fang, H. Chen, Y. Lyu, W. Broad, M. Fournier, G. Chen, Y. Hu, S. Mohammed, Q. Ling, R. P. Jarvis, Ubiquitin-based pathway acts inside chloroplasts to regulate photosynthesis. *Sci. Adv.* **8**, eabq7352 (2024).
31. G.-Z. Wu, R. Bock, GUN control in retrograde signaling: How GENOMES UNCOUPLED proteins adjust nuclear gene expression to plastid biogenesis. *Plant Cell*. **33**, 457–474 (2021).
32. J. M. Alonso, T. Hirayama, G. Roman, S. Nourizadeh, J. R. Ecker, EIN2, a bifunctional transducer of ethylene and stress responses in *Arabidopsis*. *Science* **284**, 2148–2152 (1999).
33. A. E. Hall, Q. G. Chen, J. L. Findell, G. E. Schaller, A. B. Bleecker, The relationship between ethylene binding and dominant insensitivity conferred by mutant forms of the ETR1 ethylene receptor1. *Plant Physiol.* **121**, 291–300 (1999).
34. F. An, Q. Zhao, Y. Ji, W. Li, Z. Jiang, X. Yu, C. Zhang, Y. Han, W. He, Y. Liu, S. Zhang, J. R. Ecker, H. Guo, Ethylene-induced stabilization of ETHYLENE INSENSITIVE3 and EIN3-LIKE1 is mediated by proteasomal degradation of EIN3 binding F-Box 1 and 2 that requires EIN2 in *Arabidopsis*. *Plant Cell* **22**, 2384–2401 (2010).
35. J. Zhang, Y. Chen, J. Lu, Y. Zhang, C. K. Wen, Uncertainty of EIN2Ser645/Ser924 inactivation by CTR1-mediated phosphorylation reveals the complexity of ethylene signaling. *Plant Commun.* **1**, 100046 (2020).
36. S.-D. Yoo, Y.-H. Cho, J. Sheen, *Arabidopsis* mesophyll protoplasts: A versatile cell system for transient gene expression analysis. *Nat. Protoc.* **2**, 1565–1572 (2007).
37. J. H. C. Smith, A. Benitez, Chlorophylls: Analysis in plant materials, in *Modern Methods of Plant Analysis / Moderne Methoden Der Pflanzenanalyse: Volume 4*, K. Paech, M. V Tracey, Eds. (Springer Berlin Heidelberg, Berlin, Heidelberg, 1955), pp. 142–196.
38. Q. Ling, P. Jarvis, Analysis of protein import into chloroplasts isolated from stressed plants. *J. Vis. Exp.* **117**, e54717 (2016).
39. E. W. Deutsch, N. Bandeira, Y. Perez-Riverol, V. Sharma, J. J. Carver, L. Mendoza, D. J. Kundu, S. Wang, C. Bandla, S. Kamatchinathan, S. Hewapathirana, B. S. Pullman, J. Wertz, Z. Sun, S. Kawano, S. Okuda, Y. Watanabe, B. MacLean, M. J. MacCoss, Y. Zhu, Y. Ishihama, J. A. Vizcaino, The ProteomeXchange consortium at 10 years: 2023 update. *Nucleic Acids Res.* **51**, D1539–D1548 (2023).
40. S. Okuda, Y. Watanabe, Y. Moriya, S. Kawano, T. Yamamoto, M. Matsumoto, T. Takami, D. Kobayashi, N. Araki, A. C. Yoshizawa, T. Tabata, N. Sugiyama, S. Goto, Y. Ishihama, jPOSTrepo: An international standard data repository for proteomes. *Nucleic Acids Res.* **45**, D1107–D1111 (2017).

**Acknowledgments:** We thank C.-K. Wen (Chinese Academy of Sciences) for providing the *ctr1ein2* and *ein2* mutants, C. Kim (Chinese Academy of Sciences) for supplying the *toc33* mutant, and S. Kessler (Purdue University) for sharing the GFP overexpression lines. We also acknowledge H. L. Park for assistance with this research. We are grateful for the support from the Purdue Proteomics Facility, Imaging Facility, and Electron Microscopy Facility. We thank to J. J. Kieber for providing critical comments on the manuscript. **Funding:** This work was supported by National Science Foundation funds (nos. 2245525 and 1817286) to G.M.Y. **Author contributions:** Conceptualization: G.M.Y. Methodology: G.M.Y. and Y.-C.C. Investigation: G.M.Y. and Y.-C.C. Visualization: Y.-C.C. Supervision: G.M.Y. Writing—original draft: Y.-C.C. Writing—review and editing: G.M.Y. and Y.-C.C. **Competing interests:** The authors declare that they have no competing interests. **Data and materials availability:** All data needed to evaluate the conclusions in the paper are present in the paper and/or the Supplementary Materials. The phosphite identification proteomics data have been deposited to the ProteomeXchange Consortium (39) via the jPOST partner repository (40) with the dataset identifier PXD059681 for ProteomeXchange.

Submitted 5 November 2024

Accepted 19 February 2025

Published 26 March 2025

10.1126/sciadv.adu4054